scientific reports

Check for updates

OPEN

Elevated cerebral oxygen extraction fraction in Parkinson's disease correlates with motor impairment severity

Huseyin Enes Candan[1], DongKyu Lee[2,3], Hansol Lee[4], Jae-Hyeok Lee[5], Junghun Cho[6]✉ & HyungJoon Cho[3]✉

Parkinson's disease (PD) is the second most common neurological disorder, but its diagnosis remains challenging. Cerebral glucose metabolism has emerged as a promising biomarker for PD based on previous studies. While these studies have established a PD-related pattern of metabolic activity of glucose in the brain, cerebral oxygen metabolism is less explored, and there is no well-established PD-related pattern of cerebral oxygen metabolism. This study investigates cerebral oxygen extraction fraction (OEF) as a measure of cerebral oxygen metabolism to monitor disease progression in early-stage PD. OEF was measured noninvasively using magnetic resonance imaging with the QSM + qBOLD technique in 50 PD patients and 30 healthy controls. Whole-brain and region-of-interest analyses were conducted, focusing on key regions within the basal ganglia. Results revealed significantly elevated OEF in the basal ganglia of PD patients compared to controls. Moreover, OEF showed a positive correlation with Unified Parkinson's Disease Rating Scale Part III scores, indicating an association between increased oxygen extraction and motor impairment severity in early PD. These findings support the potential of cerebral OEF as an early biomarker of motor symptom severity. Therefore, it can enhance our understanding of metabolic dysfunction in the basal ganglia during the early stages of PD.

Keywords Brain metabolism, Cerebral oxygen metabolism, Motor impairment, Oxygen extraction fraction, Parkinson's disease

Parkinson's disease (PD) is the second most common neurological disorder after Alzheimer's disease[1]. It is typically diagnosed based on the neurological examination of its motor symptoms, such as bradykinesia, resting tremor, and rigidity[1]. However, the non-specificity of these symptoms leads to a high rate of misdiagnosis, especially in the early stages of the disease[2], creating problems for patient management, prognosis, and patient selection for clinical trials[3]. To enhance early diagnostic accuracy and deepen our understanding of PD's pathophysiology, additional noninvasive biomarkers that reflect the severity of motor impairment should be explored.

Cerebral metabolic rates, measured as cerebral glucose metabolic rate (CMR_{glc}) via ^{18}F-fluoro-deoxyglucose (FDG) PET or cerebral metabolic rate of oxygen ($CMRO_2$) via ^{15}O-PET, show potential as early biomarkers of PD. PD-related metabolic pattern (PDRP)[4–8] has been established as a characteristic glucose metabolism increase in the globus pallidus, putamen, subthalamic nucleus, thalamus, cerebellum, pons, and sensorimotor cortex, along with a decrease in the lateral frontal and parietooccipital area[3,9,10]. PDRP-like oxygen metabolism increase in the basal ganglia has been observed using ^{15}O-PET[7]; however, this pattern is not well established[11]. Scarcity of ^{15}O-PET studies is likely due to difficulties of its clinical application, which is hampered by complex logistics, patient exposure to radiation, and the requirement for an on-site cyclotron to produce the ^{15}O isotope,

[1]Graduate School of Health Science and Technology, Ulsan National Institute of Science and Technology, Ulsan, Republic of Korea. [2]Korean Brain Research Institute, Brain Tech Center, Daegu, Republic of Korea. [3]Department of Biomedical Engineering, Ulsan National Institute of Science and Technology, Ulsan, Republic of Korea. [4]Department of Radiology, Athinoula A. Martinos Center for Biomedical Imaging, Massachusetts General Hospital, Charlestown, MA, USA. [5]Department of Neurology, Pusan National University School of Medicine, Pusan National University Yangsan Hospital, Yangsan, Republic of Korea. [6]Department of Biomedical Engineering, George Washington University, Washington, DC, USA. ✉email: junghunc@gwu.edu; hjcho@unist.ac.kr

which has a short half-life of 2 min[12]. Alternatively, $CMRO_2$ may be noninvasively measured using MRI with a two-step process: first, phase-contrast MRI or arterial spin labeling[13] measures cerebral blood flow (CBF), and second, T_2-relaxation-under-spin-tagging[14], quantitative susceptibility mapping (QSM)[15], or quantitative blood oxygen level dependent (qBOLD)[16] imaging measures venous oxygenation[17]. While this combination of MRI measurements provides a viable alternative to PET, oxygen extraction fraction (OEF), defined as the venous to arterial oxygenated hemoglobin concentration ratio, can be assessed independent of CBF measurements. As such, OEF may serve as a practical and informative biomarker for monitoring changes in cerebral oxygen metabolism as PD progresses as shown in previous studies[18].

On the other hand, OEF cannot be directly interpreted as a measurement of oxygen metabolism like $CMRO_2$, which is the product of OEF and CBF. Previous studies have reported unaltered CBF in the basal ganglia for PD patients compared to healthy controls, while a positive correlation between disease severity and CBF was observed[19,20]. Building on these findings, this study examines changes in OEF within the basal ganglia to determine whether abnormalities in oxygen metabolism are present in this region. Consequently, routine OEF measurement may provide valuable insights into the physiological mechanisms underlying oxygen metabolism patterns associated with PD.

While most previous studies have focused on alterations in gray matter metabolic rates, recent evidence suggests that white matter (WM) may also include markers of PD[21]. WM hyperintensities in T_2-weighted images have been reported to be closely linked with motor symptoms in PD patients. WM hyperintensities are an indicator of cerebral small vessel disease, which suggests an underlying hypoperfusion in the WM[21], which should be taken into account when interpreting OEF measurements.

In short, this study aims to investigate cerebral OEF as a potential biomarker for early to mid-stage PD. OEF was noninvasively measured using the QSM + qBOLD (QQ) method[22] with a multi-gradient-echo MRI experiment. OEF measurements were interpreted alongside previously reported CBF measurements[20] for adequate assessment of cerebral oxygen metabolism. This approach provides a deeper understanding of oxygen metabolism abnormalities in PD and explores the potential of OEF as an early biomarker for PD and its progression.

Methods

Participants

Participants were recruited from Pusan National University Yangsan Hospital (Yangsan, Republic of Korea). All participants provided informed consent in accordance with the Declaration of Helsinki. The study protocol was approved by the local institutional review board, and all methods were carried out in accordance with relevant guidelines and regulations. PD was diagnosed by an experienced neurologist (J.H.L., with 20 years of experience in movement disorders) using the UK Parkinson's Disease Society Brain Bank criteria[23]. None of the healthy control (HC) subjects had a history of head trauma, stroke, or any neurological or psychiatric illnesses.

The study included 50 patients diagnosed with PD and 30 HC participants. For the PD group, 42 participants' UPDRS-III[24] scores, Hoehn and Yahr (H-Y)[25] stages, and the Korean version of the Mini-Mental State Examination (2nd edition) (MMSE)[26] scores were assessed without requiring the withdrawal of PD medications, including levodopa or other dopamine agonists.

Magnetic resonance imaging

All participants underwent 3-T in vivo MRI (Magnetom Skyra; Siemens). A two-dimensional multi-gradient recalled echo (mGRE) sequence with six echoes was used. The echo times (TEs) were 3.1, 8.0, 13.5, 19.9, 24.4, and 30.0 ms. The repetition time (TR) was 2.03 s, scan time 6.5 min, with a flip angle of 60 degrees. The matrix size was $192 \times 192 \times 60$, with a resolution of $1 \times 1 \times 2$ mm^3 and a 0.2 mm slice gap. The imaging geometry was parallel to the anterior commissure–posterior commissure line, while covering the whole brain.

Quantitative susceptibility mapping and oxygen extraction fraction measurement

Quantitative susceptibility mapping (QSM) was performed in the native mGRE space using the morphology-enabled dipole inversion with the automatic uniform cerebrospinal fluid zero reference (MEDI + 0) algorithm[27]. Phase unwrapping was performed with Laplacian unwrapping, and background removal was performed using the projection onto dipole fields method[28] (Fig. 1). QSM + qBOLD or QQ method[29] was used for OEF mapping, which has been previously validated by comparison with ^{15}O-PET and calibrated BOLD[22] results, and has also been clinically applied to neurologic diseases[29]. With this method, OEF can be mapped without vascular challenges by utilizing both the magnitude and phase of mGRE data, a common sequence in any MRI system, making it well-suited for clinical use. This method combines QSM and qBOLD signal equations according to maximum likelihood under Gaussian noise approximation. One drawback, though, is that QQ results are highly sensitive to noise. To address this, various machine learning and deep learning algorithms have been developed[30–32], among which the latest machine learning algorithm, termed temporal clustering, tissue composition, and total variation (CCTV), was utilized in this study. CCTV first employs the cluster analysis of time evolution (CAT) method, which creates clusters based on the signal characteristics (i.e., R_2^* decay rate) and tissue type of voxels (i.e., gray or white matter). Averaging over these clusters increases the signal-to-noise ratio (SNR) and mitigates noise sensitivity. Then, CCTV applies total variation regularization to alleviate the propagation of measurement noise into the parameter map[32] (Fig. 1).

Subject registration and segmentation

T_2^*-weighted images acquired by averaging the last three echoes of mGRE images were used for the registration process. First, a preliminary linear registration was performed to create an average image using FMRIB's Linear Image Registration Tool (FLIRT) (version 6.0.7.10)[33]. Once the average image is created, all subjects' images

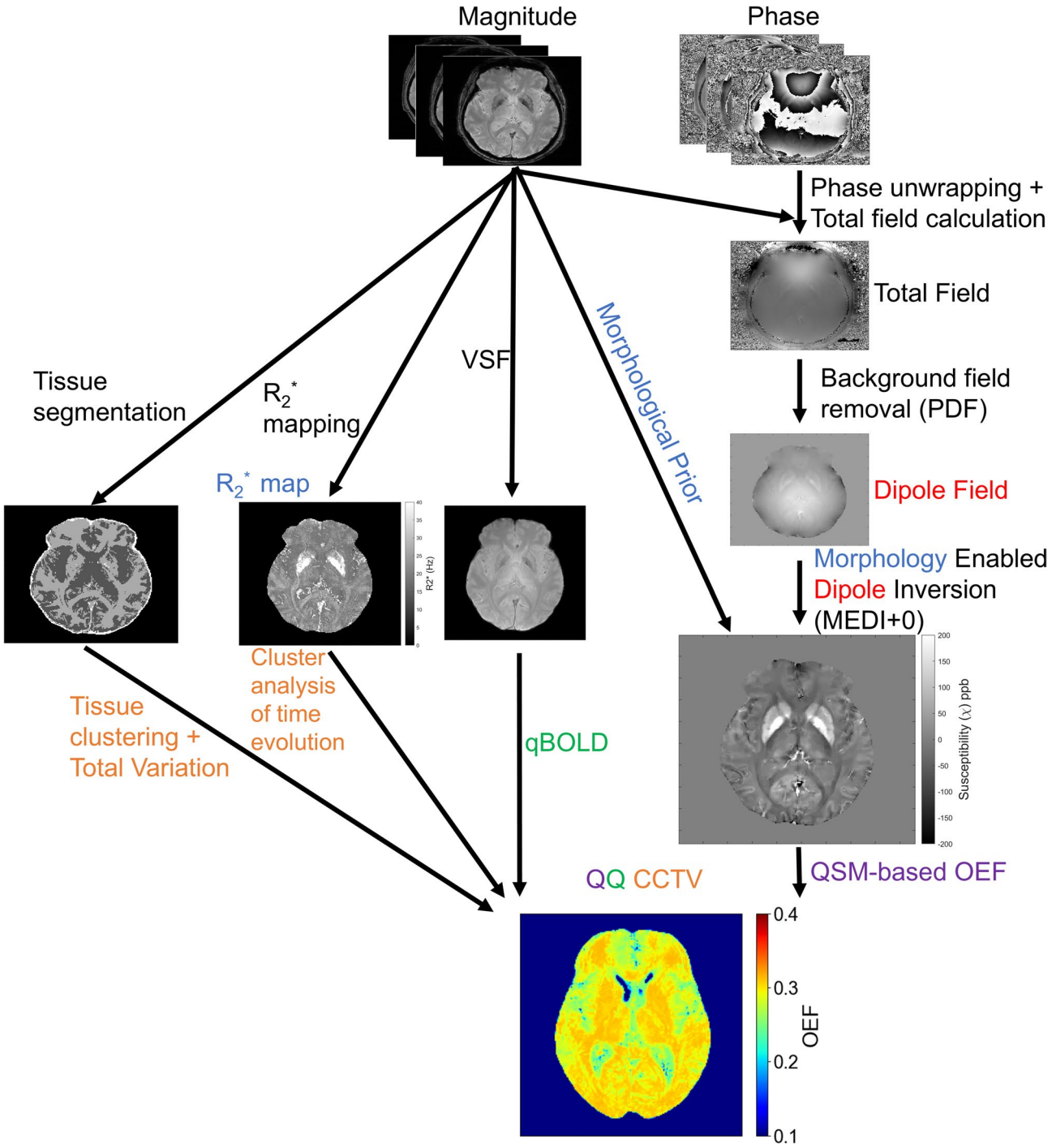

Fig. 1. Summary of the QSM and OEF mapping process. The arrows represent the flow of processing. Color coding indicates the use of that information in a particular process (e.g., the R_2^* map and magnitude images used as morphological priors in MEDI + 0.) QSM, quantitative susceptibility mapping; OEF, oxygen extraction fraction; MEDI + 0, morphology-enabled dipole inversion with an automatic uniform cerebrospinal fluid zero reference algorithm.

were registered to it with affine and nonlinear registration using FLIRT and FNIRT tools of FSL. Transformation matrices from this process were used to register OEF maps to the average image space. For the region of interest analyses, each subject's QSM was manually segmented using ITK-SNAP software (version 3.8.0)[34] as the substantia nigra (SN), red nucleus (RN), putamen, globus pallidus (GP), and caudate nucleus (CN). The same rater segmented the regions after a six-month gap, and the Dice coefficients between the segmentations were 0.8691, 0.8597, 0.8628, 0.8119, and 0.8072 for the SN, RN, putamen, GP, and CN, respectively. White matter (WM) segmentation was performed using FSL's FAST tool.

Statistical analysis

Statistical analyses were performed with MATLAB software (version 2023a; MathWorks) and Python (version 3.11, Python Software Foundation). Demographic data were compared between the HC and PD patient groups using the χ^2 test for sex and the Mann-Whitney U test for age. For the whole-brain analysis, the General Linear Model (GLM) framework in FSL was performed on the registered OEF maps. Two analyses were conducted. First, the OEF difference between the PD and HC groups was investigated. Second, the correlation between UPDRS-III scores and OEF was investigated. Age and sex were included as nuisance variables for these analyses. To reduce false positives arising from noise, voxel-wise significance maps were subjected to cluster-based thresholding where clusters smaller than 100 voxels were excluded to remove isolated voxels likely occurring by chance.

For the ROI analysis, the mean intensity of the ROIs was calculated, and then the distribution of the mean intensities in the HC and PD groups was compared using the two-tailed t-test. Normality of the distribution of the mean OEF values in the ROIs was assessed with the Anderson-Darling test. Group differences were quantified using Cohen's d, calculated as the difference in group means divided by the pooled standard deviation. For the PD group, Spearman correlation was calculated between UPDRS-III, H-Y stage, age, MMSE, and the mean OEF of the ROIs. To ensure that correlations between OEF and UPDRS-III scores were not due to the mediation of age, partial Spearman correlations were calculated with age as a control variable.

To calculate an interpretable effect size, the linear relationship between UPDRS-III and OEF was calculated with linear regression with age and sex as control variables, and the amount of OEF increase per 10 points of UPDRS-III score increase is reported. No major violations of linear regression assumptions were observed based on residual diagnostics. CBF measurements from a prior study[20] were visualized along with the OEF measurements (with permission from SAGE Publications for Pelizzari et al.[20]).

Finally, the predictive power of the mean OEF of the ROIs for classifying PD was tested using binary logistic regression. Two models were tested: first with the mean OEF values and non-blood susceptibility, and second with mean OEF values alone. The two models were tested for all participants and participants with an average of OEF < 0.3 (HC = 17, PD = 17). Model performance was evaluated with receiver operating characteristic curve (ROC) analysis. These models were validated using leave-one-out cross validation, and the overall AUC scores are reported.

Results

Demographic and clinical characteristics

The HC group included 15 male and 15 female participants, while the PD group had 27 male and 23 female participants. There were no significant differences in gender distribution between the two groups ($\chi^2(2, N = 80) = 0.32$, $p = 0.85$) (Table 1). The PD group was 5.0 years older than the control group on average ($z = -2.38$, $p = 0.017$). The mean scores of UPDRS-III (19.9 ± 6.64, mean ± std), and H-Y stage (2.08 ± 0.44, mean ± std) suggest that the enrolled PD patients were in the early to mid-stages of the disease. All participants were non-demented at the time of the study, with a mean MMSE score of 28.1 ± 1.79 (mean ± std) for the PD group.

Widespread increase of OEF in PD group correlates with motor impairment severity

OEF was significantly elevated in the key regions of the basal ganglia for the PD group (Fig. 2 and Supplementary Fig. 1 for all slices). Similarly, we have observed a correlation between UPDRS-III scores and the OEF values in widespread regions in the brain (Fig. 2). These effects were observed in the white matter and deep gray matter regions with modest effect sizes. To minimize the influence of spurious findings, only clusters exceeding a minimum size threshold of 100 voxels were retained, excluding isolated voxels likely due to chance. Notably, the spatial distribution of these clusters was not random, suggesting a systematic pattern of increased OEF associated with motor impairment severity. Therefore, we have further investigated these correlations through ROI based analysis.

Significantly higher OEF in basal ganglia and white matter

The PD group showed, on average, ~8% elevated OEF in the target ROIs compared to the HC group (Fig. 3). The ROIs were selected as key areas of the brain associated with PD, including the SN, where the difference was statistically significant (Two-tailed t-test: $t(78) = 2.07$, $p = 0.042$, $d = 0.48$). Similar significant increases in OEF were observed in the RN ($p = 0.048$, $t(78) = 2.01$, $d = 0.46$), GP ($p = 0.044$, $t(78) = 2.02$, $d = 0.47$) and putamen

	Healthy control ($n = 30$)	Parkinson's patient ($n = 50$)
Gender (Male/Female)	15/15	27/23
Age (mean ± std)	56.4 ± 10.9	61.4 ± 4.2*
Disease duration (year) (mean ± std)		5.4 ± 3.8
H-Y Stage		2.08 ± 0.44
UPDRS-III (Motor Eval)		19.9 ± 6.64
MMSE		28.1 ± 1.97

Table 1. Summary of participant demographics. H-Y stage, UPDRS-III and MMSE scores are available for 42 patients. *$p < 0.05$.

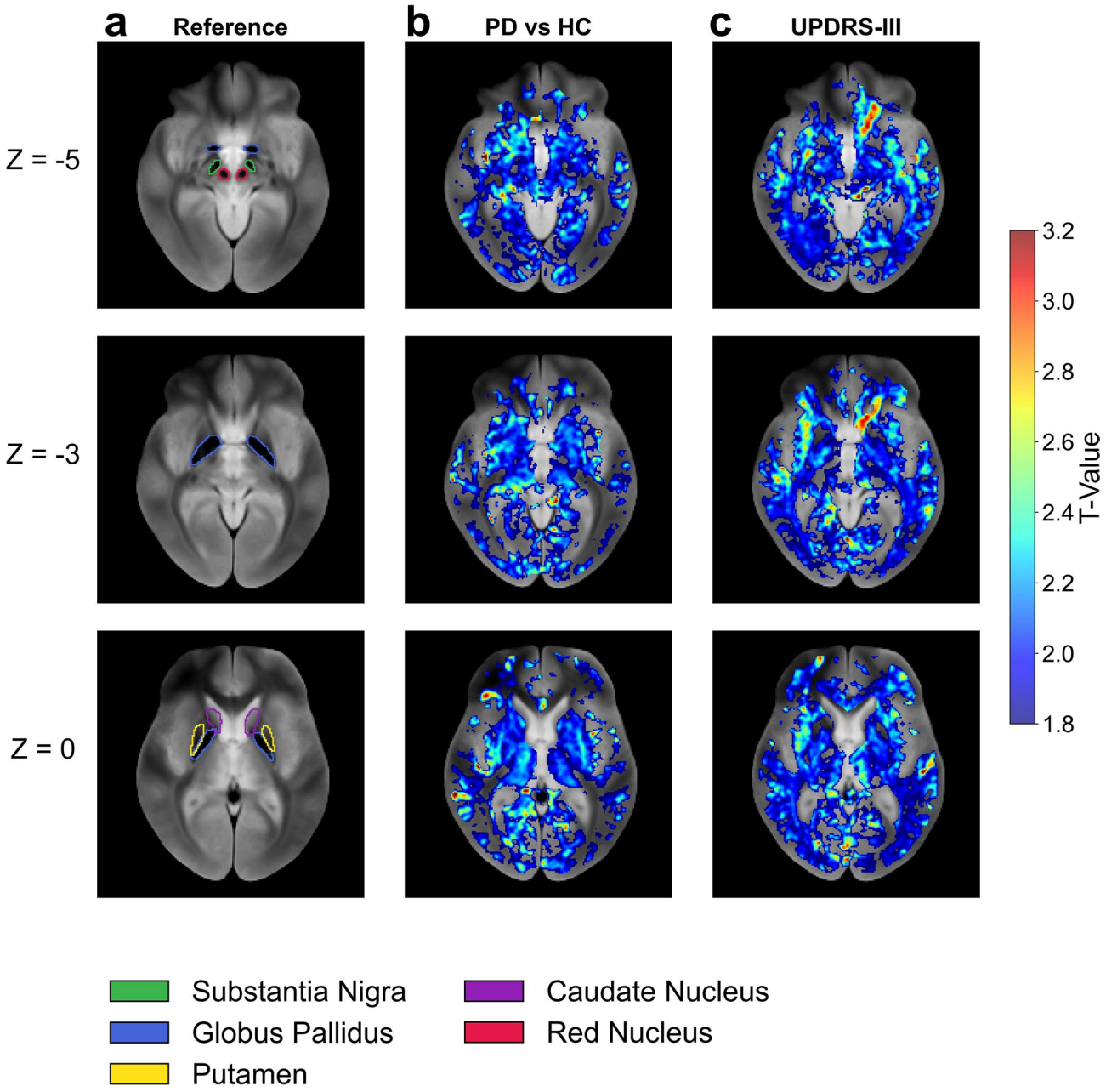

Fig. 2. Results of whole-brain analysis. (A) Anatomical reference is shown with regions of interest in colored outlines. Three slices are shown at positions Z = -5, -3, 0 in reference to the average subject origin. (B) Regional differences in OEF between PD and HC groups where T > 0 indicates PD > HC. Age and sex have been included as nuisance variables. (C) OEF of regions that are correlated with UPDRS-III scores where T > 0 indicates positive correlation between UPDRS-III scores and OEF. Age and sex have been included as nuisance variables. Only $p < 0.05$ is shown. Only clusters exceeding a minimum size threshold of 100 voxels were retained. OEF, oxygen extraction fraction; PD, Parkinson's disease; HC, healthy control.

($p = 0.048$, t(78) = 2.01, d = 0.46) with CN ($p = 0.07$, t(78) = 2.03, d = 0.42) and WM ($p = 0.10$, t(78) = 1.66, d = 0.38) showing marginal significance, although effect sizes were moderate (Supplementary Table 1). The findings suggest that these critical regions show higher metabolic activity or altered oxygen utilization in PD patients.

Positive correlation between PD metrics and OEF

The OEF values in the SN, RN, GP, and WM positively correlated with UPDRS-III motor scores ($p < 0.05$), with Spearman correlation coefficients ranging from 0.330 to 0.341 (Fig. 4A-B). These relationships remained significant after controlling for age (Table 2). OEF increased by an average of 1.6% in RN, SN, GP, and WM per 10 points increase in UPDRS-III scores. OEF in the putamen also showed a positive trend with UPDRS-III ($\rho = 0.288$), but this did not reach statistical significance, indicating a marginal relationship ($p < 0.1$). Similarly,

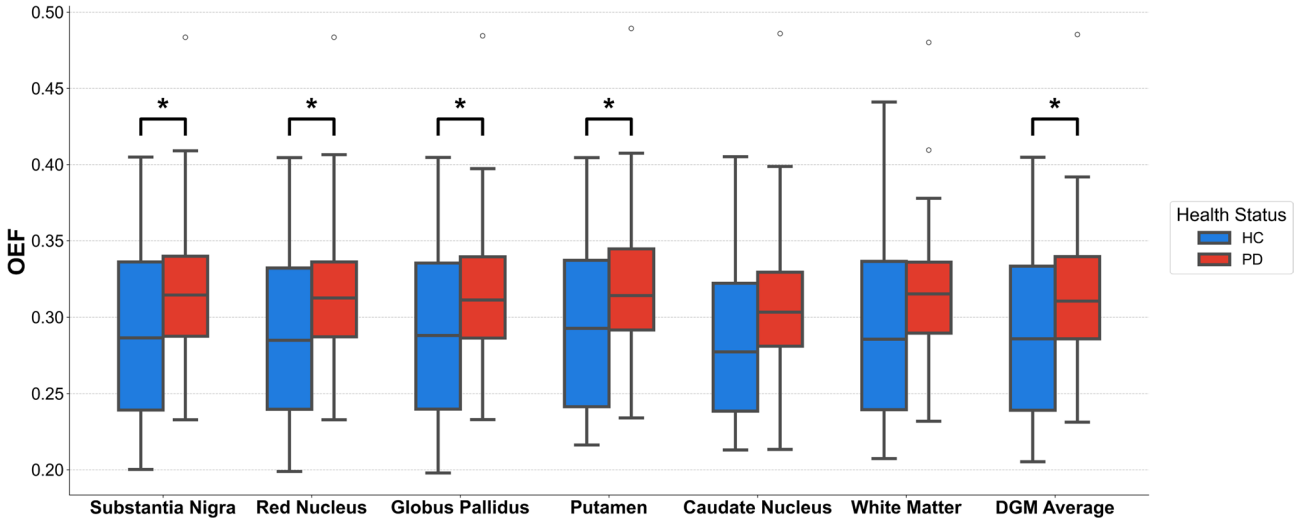

Fig. 3. Group level comparison with the two-tailed t-test results of OEF in each ROI ($n = 50$ for PD, and $n = 30$ for HC). Asterisk "*" indicates $p < 0.05$. OEF, oxygen extraction fraction; PD, Parkinson's disease; ROI, region of interest; HC, healthy control; DGM, deep gray matter.

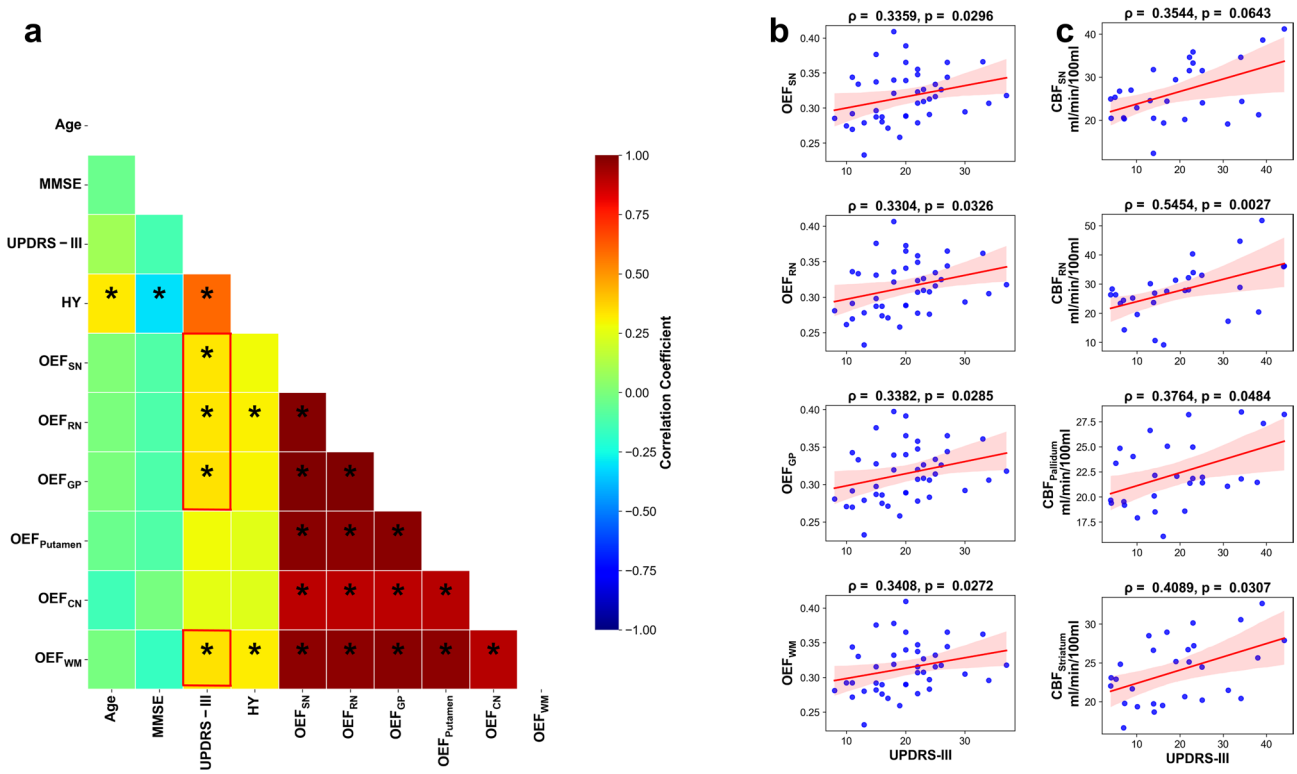

Fig. 4. Results of correlation analysis. (**A**) Correlation table showing the Spearman correlation between patient metrics and OEF values in the selected ROIs. The asterisk represents $p < 0.05$, and the red outline highlights the significant and marginally significant correlations between OEF measures and UPDRS-III. (**B**) Highlighted correlations with the red rectangle in panel A are presented as scatter plots. ($n = 42$ for PD) (**C**) CBF vs. UPDRS-III relationship based on the data from (Pelizzari, Laganà et al.)[20]. CBF measurements from a prior study by Pelizzari et al.[20] were adapted from Fig. 2 of the original publication with permission from SAGE Publications and are plotted for comparison. OEF, oxygen extraction fraction; PD, Parkinson's disease; ROI, region of interest; CBF, cerebral blood flow.

Metric		Age	MMSE	UPDRS-III	H-Y Stage
OEF	SN	0.014, $p=0.931$	-0.109, $p=0.494$	0.336 (0.336), $p=0.030^*$ (0.032^*)	0.282, $p=0.070$
	RN	-0.0004, $p=0.998$	-0.110, $p=0.486$	0.330 (0.332), $p=0.033^*$ (0.034^*)	0.309, $p=0.046^*$
	GP	-0.001, $p=0.994$	-0.117, $p=0.460$	0.338 (0.340), $p=0.028^*$ (0.030^*)	0.298, $p=0.049^*$
	Putamen	-0.044, $p=0.781$	-0.104, $p=0.511$	0.288 (0.294), $p=0.064$ (0.062)	0.244, $p=0.119$
	CN	-0.143, $p=0.365$	-0.015, $p=0.924$	0.250 (0.268), $p=0.110$ (0.091)	0.235, $p=0.134$
	White Matter	-0.011, $p=0.947$	-0.165, $p=0.295$	0.341 (0.343), $p=0.027^*$ (0.028^*)	0.313, $p=0.044^*$

Table 2. Spearman correlations between OEF values in selected rois and patient Age, MMSE, UPDRS-3, and H-Y stage for the PD group. Partial correlations (with age and MMSE as control variables) are shown in parenthesis. *: $p<0.05$.

CN also showed a positive trend with no statistical significance. Additionally, a consistent pattern of positive correlation was noted between OEF and H-Y stage, although only the RN and WM regions reached significance (asterisk-marked, Fig. 4A), suggesting that OEF elevations in the basal ganglia may track disease progression.

To assess the hemodynamic relevance of these metabolic findings, we have compared the relationship between UPDRS-III scores and CBF values in regions using previously published data from Pelizzari et al.[20] (Fig. 4C, with permission from SAGE Publications). Their analysis shows similar positive correlations between CBF and UPDRS-III in SN, RN, and GP ($\rho = 0.35–0.55$), reinforcing the link between regional metabolic demand and clinical severity in PD. The converging patterns between increased OEF and CBF with worsening motor symptoms support the hypothesis of region-specific metabolic compensation or vascular dysregulation in the basal ganglia circuitry. Collectively, these findings underscore the clinical relevance of OEF alterations in PD and suggest that OEF, particularly in SN, RN, and GP, may serve as a sensitive biomarker for motor symptom severity.

Predictive power of OEF for classification

ROC analysis for the binary logistic regression models revealed low predictive power with an area under the ROC curve (AUC) values of around 0.65 (cross-validation results around 0.58) (Supplementary Fig. 2). While adding non-blood susceptibility as a variable marginally increased the model's predictive power, this is likely due to overfitting with the two variable model based on leave-one-out cross validation results (Supplementary Table 2). Overall, this suggests that even though OEF is elevated in the PD group, it is insufficient to classify PD. However, these models worked relatively well when classifying the PD and HC groups for subjects with average OEF less than 0.3, with AUC values of 0.78 (cross-validation AUC = 0.75) in the SN. Possibly due to the wider distribution of OEF values for the HC group.

Discussion

We have investigated OEF as an early biomarker for PD. Results show that OEF is not only elevated in early to mid-stage PD patients (UPDRS-III = 19.9 $\pm$ 6.64, durations = 5.4 $\pm$ 3.8) but also correlates with UPDRS-III scores, showing its ability to reflect the severity of motor impairment. Therefore, OEF can provide insight into the onset and progression of PD. To the best of our knowledge, this is the first observation of a positive correlation between OEF and movement symptom severity in early-stage PD.

When analyzed in tandem with previously reported CBF measurements, our OEF measurements support the presence of a PDRP-like pattern[9,35,36] manifesting as oxygen hypermetabolism in the basal ganglia of early PD patients, in agreement with previous papers[7,18]. This metabolic pattern may reflect the characteristic changes in brain oxygen metabolism that occur due to the loss of dopaminergic neurons and the resulting disruption of neural circuits in PD. Though hypermetabolism in the basal ganglia was well established for glucose metabolism, there are conflicting studies for oxygen metabolism[11,37]. Our results, along with previous evidence reporting unaltered perfusion in the basal ganglia[19,20] in PD patients compared to healthy controls, favor the idea that oxygen metabolism, like glucose metabolism, increases in the early stages of PD in the basal ganglia. Moreover, current evidence shows that motor impairment severity correlates with both perfusion[20] and OEF, suggesting a positive correlation between oxygen metabolic rates and motor impairment severity in the early stages of the disease. The coupled increase in glucose and oxygen metabolism may signify an aerobic respiration anomaly, possibly an inefficiency in the mitochondria due to oxidative stress.

Unlike our findings in the deep gray matter, the observed increase in OEF within WM may reflect hypoperfusion, increased oxygen metabolism, or a combination of both, given the prior evidences[21,38]. According to these studies, it is likely that hypoperfusion is the primary cause of the correlation between UPDRS-III scores and OEF in the WM, since markers of hypoperfusion were reported to be highly correlated with motor impairment severity[21]. However, WM is not as extensively investigated as gray matter and is only recently gaining attention[21], and whether the observed effect is due to hypoperfusion or increased oxygen metabolism requires perfusion measurements. Therefore, a complete understanding of oxygen metabolism in WM in PD requires further research.

There are limitations to this study. First, the PD group was on average 5 years older than the HC group. To account for this, we have included age as a covariate during the whole-brain GLM analyses and calculated the partial correlation coefficients for ROI analyses to control for age. Our results show that the observed relationship between UPDRS-III scores and OEF was not mediated by age. However, the age difference between groups represents a limitation, as residual confounding may remain. Second, the uniform nature of OEF[39] across the brain complicates distinguishing metabolic rate differences in the ROIs, because an overall increase in cerebral OEF could mask regional variations. However, given the prior evidence showing increased CBF in basal ganglia regions, our results signify an increased oxygen metabolism in these regions for early PD patients. Third, the lack of perfusion measurements makes it difficult to interpret the relationship between OEF measurements and true metabolic changes. Moreover, the observed correlation between OEF and motor impairment severity was modest, and OEF alone showed low diagnostic classification, limiting its strength as a standalone biomarker. Fourth, participants in the study were not withdrawn from PD medications and levodopa equivalent daily dose (LEDD) was not calculated. Given that there is previous evidence suggesting a relationship between dopamine agonists and cerebral oxygen metabolism[40], this should be controlled in future studies.

In summary, although further research with perfusion measurements and longitudinal designs is necessary to fully understand the biological mechanisms responsible for the observed increase in cerebral OEF in PD patients, this study demonstrates the potential of cerebral OEF as a noninvasive and convenient biomarker for PD, which reflects motor impairment severity. Based on these findings, OEF may offer valuable insights into the oxygen metabolism in PD and its relationship with motor impairment severity.

Data availability

The datasets used and/or analyzed during the current study available from the corresponding author on reasonable request.

Received: 28 October 2025; Accepted: 13 January 2026
Published online: 18 January 2026

References

1. Bloem, B. R., Okun, M. S. & Klein, C. Parkinson's disease. *Lancet* **397**, 2284–2303 (2021).
2. Beach, T. G. & Adler, C. H. Importance of low diagnostic accuracy for early parkinson's disease. *Mov. Disord.* **33**, 1551–1554 (2018).
3. Meles, S. K., Teune, L. K., de Jong, B. M., Dierckx, R. A. & Leenders, K. L. Metabolic imaging in Parkinson disease. *J. Nucl. Med.* **58**, 23–28 (2017).
4. Wu, P. et al. Metabolic brain network in the Chinese patients with parkinson's disease based on 18F-FDG PET imaging. *Parkinsonism Relat. Disord.* **19**, 622–627 (2013).
5. Wolfson, L. I., Leenders, K. L., Brown, L. L. & Jones, T. Alterations of regional cerebral blood flow and oxygen metabolism in parkinson's disease. *Neurology* **35**, 1399–1399 (1985).
6. Lin, T. P. et al. Metabolic correlates of subthalamic nucleus activity in parkinson's disease. *Brain* **131**, 1373–1380 (2008).
7. Powers, W. J. et al. Cerebral mitochondrial metabolism in early parkinson's disease. *J. Cereb. Blood Flow. Metabolism.* **28**, 1754–1760 (2008).
8. Matthews, D. C. et al. FDG PET parkinson's disease-related pattern as a biomarker for clinical trials in early stage disease. *NeuroImage: Clin.* **20**, 572–579 (2018).
9. Teune, L. K. et al. Parkinson's disease-related perfusion and glucose metabolic brain patterns identified with PCASL-MRI and FDG-PET imaging. *NeuroImage: Clin.* **5**, 240–244 (2014).
10. Teune, L. K. et al. Validation of parkinsonian disease-related metabolic brain patterns. *Mov. Disord.* **28**, 547–551 (2013).
11. Borghammer, P. et al. Cerebral oxygen metabolism in patients with early parkinson's disease. *J. Neurol. Sci.* **313**, 123–128 (2012).
12. Jiang, D. & Lu, H. Cerebral oxygen extraction fraction MRI: techniques and applications. *Magn. Reson. Med.* **88**, 575–600 (2022).
13. Buxton, R. B. Quantifying CBF with arterial spin labeling. *J. Magn. Reson. Imaging.* **22**, 723–726 (2005).
14. Lu, H. et al. Calibration and validation of TRUST MRI for the Estimation of cerebral blood oxygenation. *Magn. Reson. Med.* **67**, 42–49 (2012).
15. Zhang, J. et al. Quantitative susceptibility mapping-based cerebral metabolic rate of oxygen mapping with minimum local variance. *Magn. Reson. Med.* **79**, 172–179 (2018).
16. He, X., Yablonskiy, D. A. & Quantitative, B. O. L. D. Mapping of human cerebral deoxygenated blood volume and oxygen extraction fraction: default state. *Magn. Reson. Medicine: Official J. Int. Soc. Magn. Reson. Med.* **57**, 115–126 (2007).
17. Xu, F., Ge, Y. & Lu, H. Noninvasive quantification of whole-brain cerebral metabolic rate of oxygen (CMRO2) by MRI. *Magn. Reson. Med.* **62**, 141–148 (2009).
18. Yan, S. et al. Spatiotemporal patterns of brain iron-oxygen metabolism in patients with parkinson's disease. *Eur. Radiol.* **34**, 3074–3083 (2024).
19. Melzer, T. R. et al. Arterial spin labelling reveals an abnormal cerebral perfusion pattern in parkinson's disease. *Brain* **134**, 845–855 (2011).
20. Pelizzari, L. et al. Cerebral blood flow and cerebrovascular reactivity correlate with severity of motor symptoms in parkinson's disease. *Ther. Adv. Neurol. Disord.* **12**, 1756286419838354 (2019).
21. Yang, K. et al. White matter changes in parkinson's disease. *Npj Parkinson's Disease*. **9**, 150 (2023).
22. Cho, J., Ma, Y., Spincemaille, P., Pike, G. B. & Wang, Y. Cerebral oxygen extraction fraction: comparison of dual-gas challenge calibrated BOLD with CBF and challenge-free gradient echo QSM + qBOLD. *Magn. Reson. Med.* **85**, 953–961 (2021).
23. Hughes, A. J., Daniel, S. E., Kilford, L. & Lees, A. J. Accuracy of clinical diagnosis of idiopathic parkinson's disease: a clinico-pathological study of 100 cases. *J. Neurol. Neurosurg. Psychiatry*. **55**, 181–184 (1992).
24. Goetz, C. G. et al. Movement disorder Society-sponsored revision of the unified parkinson's disease rating scale (MDS-UPDRS): scale presentation and clinimetric testing results. *Mov. Disorders: Official J. Mov. Disorder Soc.* **23**, 2129–2170 (2008).
25. Hoehn, M. M. & Yahr, M. D. Parkinsonism: onset, progression, and mortality. *Neurology* **17**, 427–427 (1967).
26. Arevalo-Rodriguez, I. et al. Mini-Mental State Examination (MMSE) for the early detection of dementia in people with mild cognitive impairment (MCI). *Cochrane Database Syst. Rev.* (2021).
27. Liu, T. et al. Morphology enabled dipole inversion (MEDI) from a single-angle acquisition: comparison with COSMOS in human brain imaging. *Magn. Reson. Med.* **66**, 777–783 (2011).
28. Liu, T. et al. A novel background field removal method for MRI using projection onto dipole fields. *NMR Biomed.* **24**, 1129–1136 (2011).

29. Cho, J. et al. Cerebral oxygen extraction fraction (OEF): comparison of challenge-free gradient echo QSM + qBOLD (QQ) with 15O PET in healthy adults. *J. Cereb. Blood Flow. Metabolism*. **41**, 1658–1668 (2021).
30. Cho, J. et al. QQ-NET – using deep learning to solve quantitative susceptibility mapping and quantitative blood oxygen level dependent magnitude (QSM + qBOLD or QQ) based oxygen extraction fraction (OEF) mapping. *Magn. Reson. Med.* **87**, 1583–1594 (2022).
31. Cho, J. et al. Cluster analysis of time evolution (CAT) for quantitative susceptibility mapping (QSM) and quantitative blood oxygen level-dependent magnitude (qBOLD)-based oxygen extraction fraction (OEF) and cerebral metabolic rate of oxygen (CMRO2) mapping. *Magn. Reson. Med.* **83**, 844–857 (2020).
32. Cho, J., Spincemaille, P., Nguyen, T. D., Gupta, A. & Wang, Y. Temporal clustering, tissue composition, and total variation for mapping oxygen extraction fraction using QSM and quantitative BOLD. *Magn. Reson. Med.* **86**, 2635–2646 (2021).
33. Jenkinson, M., Beckmann, C. F., Behrens, T. E., Woolrich, M. W. & Smith, S. M. *Fsl Neuroimage* **62**, 782–790 (2012).
34. Yushkevich, P. A., Gao, Y. & Gerig, G. In *38th Annual International Conference of the IEEE Engineering in Medicine and Biology Society (EMBC)* 3342–3345 (IEEE, 2016).
35. Tang, C. C., Poston, K. L., Dhawan, V. & Eidelberg, D. Abnormalities in metabolic network activity precede the onset of motor symptoms in parkinson's disease. *J. Neurosci.* **30**, 1049–1056 (2010).
36. Tang, B. L. Glucose, glycolysis, and neurodegenerative diseases. *J. Cell. Physiol.* **235**, 7653–7662 (2020).
37. Kitamura, S. et al. Cerebral blood flow and oxygen metabolism in patients with parkinson's disease. *No Shinkei = Brain Nerve*. **40**, 979–985 (1988).
38. Wang, M. et al. White matter microstructural alterations and brain metabolism distributions in parkinson's disease. *Brain Imaging Behav.* **2025**, 1–11 (2025).
39. Hyder, F. et al. Uniform distributions of glucose oxidation and oxygen extraction in Gray matter of normal human brain: no evidence of regional differences of aerobic Glycolysis. *J. Cereb. Blood Flow. Metabol.* **36**, 903–916 (2016).
40. Ko, J. H., Lerner, R. P. & Eidelberg, D. Effects of Levodopa on regional cerebral metabolism and blood flow. *Mov. Disord.* **30**, 54–63 (2015).

Author contributions

H.E.C. processed and conducted statistical analysis on the MRI data and wrote the first draft of the manuscript. D.L. performed the registration of MR images. H.L. and J.L. were responsible for acquiring MRI data and UPDRS-III scores. J.C. implemented the QQ-CCTV code. H.C. conceptualized the study and interpreted the results. All authors contributed to writing the manuscript and approved the final manuscript.

Funding

This research was supported by a grant from the Korea Dementia Research Project through the Korea Dementia Research Center (KDRC), funded by the Ministry of Health & Welfare and the Ministry of Science and ICT, Republic of Korea (grant number: RS-2024-00334574). This work was partially supported by grants from the National Research Foundation of Korea of the Korean government (RS-2025-02216928).

Declarations

Competing interests

The authors declare no competing interests.

Ethical approval

This study protocol was approved by the institutional review board of the Pusan National University Yangsan Hospital (Yangsan, Republic of Korea).

Additional information

Supplementary Information The online version contains supplementary material available at https://doi.org/10.1038/s41598-026-36435-z.

Correspondence and requests for materials should be addressed to J.C. or H.C.